Diluent effects on the stability range of w/o micellar systems and microemulsions made with anionic extractants

Asmae El Maangar, Tobias Lopian, Sandrine Dourdain, Werner Kunz, Thomas Zemb

EPJ Nuclear Sci. Technol. **8**, 28 (2022)

https://doi.org/10.1051/epjn/2022025

EPJ Nuclear Sciences & Technologies

Available online at:
https://www.epj-n.org

REGULAR ARTICLE

OPEN ACCESS

Diluent effects on the stability range of w/o micellar systems and microemulsions made with anionic extractants

Asmae El Maangar[1], Tobias Lopian[1,2], Sandrine Dourdain[1], Werner Kunz[2], and Thomas Zemb[1*]

[1] ICSM, University of Montpellier, CEA, CNRS, ENSCM, Marcoule, France
[2] Institute of Physical and Theoretical Chemistry, University of Regensburg, D-93040 Regensburg, Germany

Received: 18 November 2021 / Received in final form: 20 June 2022 / Accepted: 14 September 2022

Abstract. Here we present a series of complete phase prisms for water, an organic diluent and di-(2-ethylhexyl) phosphoric acid (HDEHP), one of the most widely used double-branched lipophilic surfactants in hydrometallurgy. Partial or total titration with sodium hydroxide evidence that the mole fraction of the counter-cation "Z" is the variable that controls the packing and spontaneous curvature of the curved film formed by this extractant. Penetrating solvents such as toluene and iso-octane and the non-penetrating solvent dodecane as well as common hydrotropes acting as co-solvents, are considered. The three classical cuts of the phase prism are shown. The regions for which liquid–liquid extraction is possible are determined, as well as the location of the liquid crystals at the origin of the often observed third-phase formation. It is shown that profoundly different trends are obtained when replacing the common solvents currently used in hydrometallurgical processes with hydrotropes.

1 Introduction

Phase diagrams are commonly used to check the macroscopic consequences of the microstructures at equilibrium, obtained for different compositions of ternary or quaternary systems containing at least one surface-active agent (surfactant). Such phase diagrams are necessary to optimize the formulation of any complex fluid involved in liquid–liquid extraction processes [1]. In the context of chemical engineering, the solvent in which the surfactant is soluble is often called the diluent, and the surfactant is called the extractant. For homogeneity, we keep these terms extractant and diluent. The term solvent in this paper refers to a phase containing a mixture of extractant and diluent. In other words, it refers to an organic phase.

In the field of cosmetics and household products, the most useful phase diagrams were collected twenty years ago in a reference handbook [2]. When hydrotropes or short-chain surfactants are used instead of classical surfactants, weakly associated structures are obtained. In this case, the phase diagram is simplified, as the liquid crystalline phases disappear and most of the time, only one critical point is found around the water-oil miscibility gap [3].

Micelles and microemulsions are similarly reported as monophasic domains in the phase diagrams. Microemulsions differ from micelles by the presence of "internal" fluid, whereas micelles are formed from a curved mixed film only (i.e., without any "internal" fluid) [4]. In this sense, most "reverse" water in oil aggregates (w/o) delaminated by a strongly curved interfacial film is indeed microemulsions when the mole ratio of water to extractant is above 6–8. Conversely, when less than 6 water molecules per extractant are present, all water is immobilized as a first hydration layer of the extractant: reverse micelles have a polar core but no internal fluid with higher mobility than the extractant [5]. The intrinsic fast movement is detectable experimentally when the water-to-extractant mole ratio is above 6–8. Below this value, the solution, more specifically, is considered a reverse micellar solution since all the "inner" water is bound to the head groups and has no intrinsic faster diffusion than the extractant film.

At high extractant concentrations, and even more in the case of a rigid extractant film, lyotropic liquid crystals are present in phase triangles [6]. In the phase diagrams, the distinction between solutions containing only monomers and monomers coexisting with reverse micelles and microemulsions with free inner water is not made since there is no phase transition boundary. The liquid samples without long-range order are traditionally numbered L1 in the water corner of the phase diagram, L2 in the diluent corner of the phase diagram, and when present in some specific ratios L3 and even L4 [7].

The chemical nature of the polar head-group that binds the water molecules has a profound influence on the

* e-mail: thomas.zemb@icsm.fr

phase diagram, whereas the elastic properties are defined by the length and flexibility of the hydrocarbon chains [5]. Hydrated polar headgroups are at the origin of the repulsive hydration force coming from water molecules bound at the interface [8]. The resistance to bending of the extractant film away from the preferred spontaneous curvature limits the amount of diluent or water embedded in the microstructure, still forming a single phase (called Winsor-IV in the early literature) [9].

In hydrometallurgy, extraction, refining, and recycling of metals are always carried out in a stable coexistence of an aqueous (or water-rich) phase and a diluent-rich phase. The formation of a "third" phase, corresponding in the phase diagram to a triangle surrounded by regions of two-phase equilibria, must be avoided at any cost when liquid–liquid extraction is to be performed. The regions of two-phase coexistence without the presence of thick interphase in a phase diagram were initially called "Winsor-II" type equilibrium in the context of oil extraction [10]. In the context of metal extraction, a diluent phase containing as much as possible of extractant is contacted to an aqueous solution containing the metal to be extracted, but also other undesired metals. The metals of interest should be extracted, while the other metals should remain in the aqueous phase [11]. The driving force for ion transfer is the specific interaction with several extractants, but also entropy and local solvent structure [12].

In hydrometallurgical processes related to the nuclear fuel cycle, almost all metals of the periodic table are present simultaneously as fission products in coexistence with uranium, americium, curium, and plutonium in a highly acidic solution. In this case, large performance improvements and waste reduction can be achieved by adding phase modifiers. Due to its miscibility with oil and analogy with hydrotropes used for solubilization in water, octanol has been considered a "lipotrope". Typically, 5% of octanol is added to the main solvent-rich phase containing already the extractant molecules and alkane used as diluent. This allows a higher metal load to be extracted [13]. When the additive used is also a co-solvent, the resulting process is called ATPS (i.e., Aqueous Two-Phase System). A co-solvent is a molecule that is added to a mixture of separate substances that are typically immiscible in order to increase their solubility.

This case has been described by Rodgers et al. [14] as well as by Larpent et al. [15]. There is no longer a complete separation between a water-miscible diluent and a highly "hydrophobic" diluent. The solvent phase, in this case, contains less than one water molecule per extractant, while the water-rich phase contains less than 1% of the extractant that must be re-extracted before passing into the effluent stream. The region of the ternary phase diagram used still involves an extractant-rich and an extractant-poor phase, and care must be taken with the hydrotropic transfer. In all cases, the full phase prism must be determined in order to optimize processes and avoid third-phase formation and regions where excessive viscosity drastically reduces the efficiency of liquid–liquid extraction [16].

In the nuclear fuel cycle, phosphorus-based extractants are widely used. The exact phase diagrams depend on the purity of the extractant considered and are industry secrets [17]. Phase diagrams also depend on the purity of the solvents available at an industrial scale, as well as on the presence of radiolytic residues from solvent or extracted water. For example, tributyl phosphate (TBP), a very important compound in the nuclear industry, can be degraded to dibutyl phosphate (DBP) or monobutyl phosphate (MBP), which leads to decreased extraction performances. Special sections of plants devoted to solvent regeneration are then necessary. But it is also necessary to prepare phase maps with different ratios of degraded extractant [18,19]. The complete phase prism available in open literature describes stability compositions for diamide-based extractants [20]. In the western world, tributyl phosphate, which was discovered serendipitously during the Manhattan project [21], is still the main extractant in nuclear fuel recycling.

Considering liquid–liquid extraction outside of the nuclear field, the efficient, cheap, and widely used extractant bis(2-ethylhexyl) sulfosuccinate sodium salt "AOT" is by far the most studied and described extractant [22–25]. Four key properties are responsible for the great attention paid to AOT:

- the presence of a very small amount of water is required to nucleate the reverse micelles that perform the extraction [26]. No reverse micelles are detected in the complete absence of water.
- Two branched chains close to iso-octane are present. This ensures low resistance to curvature variation of the formed nanostructures: water-rich and diluent-rich micelles can be present at the same temperature in a ternary phase prism [23,24].
- The octyl chains are branched, this introduces an important entropic term in the free energy of aggregate formation [27]. The easy formation of aggregates contributes to the high free energy of transfer of "wanted" versus "unwanted" species since the micellization and curvature energies are minimized. One consequence is that aggregates with vanishing curvature can be formed. There are large domains of lamellar phases in the phase triangle at any temperature, as noticed by Kunieda and Shinoda when iso-octane is used as a diluent [28]. When the non-penetrating decane is used as a diluent, the extension of the lamellar phase is reduced, a hexagonal liquid crystal appears, and water-rich and diluent-rich phases coexist [29]. In iso-octane, the presence of a small but controlled amount of salt can tune the temperature at which spontaneous curvature is exactly zero [30].
- The area per molecule, and thus the spontaneous curvature is very sensitive to the electrostatic screening. Direct (o/w), reverse micelles, water-in-oil microemulsions, as well as lamellar phases can be obtained without even using a co-surfactant or mixing extractants to adjust the curvature. Large stability domains of microemulsions coexist with swollen lamellar phases.

It turns out that a phosphate-based analog of AOT exists and has great potential interest for formulations [31,32], especially when used in synergy with another more conventional extractant [33–39]. A mixture of AOT and one of

its analogs have been shown to be of excellent efficiency in nuclear fuel cycles [33,40]. This molecule is the well-described di-(2-ethylhexyl) phosphoric acid (HDEHP). More than 200 papers mention its use in liquid–liquid extraction. They describe some measurements of selective separation between species but do not contain full information on the stability as a function of the composition of the solutions studied. However, the extent of the Winsor II domain as well as the absence of liquid crystalline phases close to the compositions used in practice, must be known to obtain an efficient extraction without the risk of the third phase formation.

The aim of this work is to make the phase diagrams of complex fluids, consisting of HDEHP, water, and diluents at room temperature, accessible to engineers and physical chemists, in order to facilitate the use of HDEHP in recycling processes. Showing the ternary phase diagram of HDEHP only in its purely acidic form is not representative and would be of no practical interest. Phase triangles are useful in formulation when represented as a prism, with the variable controlling the curvature taken as one of the axes of the prism. The efficient control of the spontaneous curvature of the extractant film was first reported in a seminal paper twenty years ago [41]. There are several ways to control the spontaneous curvature of a surfactant (or extractant) film by formulation. In the case of ethoxylated surfactants, the axis related to curvature is temperature. In the case of AOT, the way to modify the curvature is to add salt, which reduces the surface area per head group. In the case of the diethyl hexyl phosphate, considered an amphiphilic anion, the most general and reliable way to control the spontaneous curvature of the extractant film is the mole fraction of sodium ions replacing the acid protons of HDEHP. This variable is labeled Z in the following [42]. Z is easily controlled by partial titration of a reverse micellar solution by sodium hydroxide. This fundamental variable Z controlling the curvature is taken as the axis of the prism, obtained by stacking triangles made for different values of the spontaneous curvature. Note that in engineering literature, HLD (i.e., Hydrophilic Lipophilic Difference) and HLD-NAC (i.e., Hydrophilic Lipophilic Difference – Net Average Curvature) are sometimes used in a similar way to describe curvature [43–47]. A general discussion of cuts in phase diagrams with the x-axis being the tuned curvature can be found in classical references [48,49].

In our case, the face of the prism with $Z = 0$ is the triangle corresponding to pure HDEHP, and the bottom face with $Z = 1$ corresponds to the NaDEHP/water/diluent phase diagram.

2 The different phase diagrams and cuts through them

In order to produce a representative phase prism, sodium has been chosen as a counter-ion. For the sodium counterion, we ion-exchange the desired quantity of protons following the procedure of Paatero [1,50,51]. We use sodium hydroxide as a neutralization agent, thus forming NaDEHP. The sodium form of HDEHP has been extensively analyzed in previous studies in terms of its phase behavior [52–54], aggregation [55–57], dynamic properties [58], conductivity [22], and interfacial properties [59]. Additionally, the branched double-strand nature of NaDEHP is close to the molecular structure of a benchmark surfactant: Aerosol OT (AOT). Both molecules possess two 2-ethylhexyl chains. AOT was the first extractant for which the extraction of free energy of amino acids has been quantitatively measured and theoretically predicted [60,61]. Due to the branching of the chains and the resulting flexibility of the surfactant film [62], they are classified in the amphiphile class of hyper-branched surfactants, which are able to form microemulsions without the addition of further additives [23,24,63].

NaDEHP is extremely hygroscopic and must be stored in the presence of a drying agent. Phase diagrams are determined by preparing typically 60–100 samples spaced in phase prisms. The exact location of phase boundaries is determined by slow titration and a visual inspection: when water or diluent is added, the sample becomes turbid and two-phase regions are detected by the persistence of clouding. The presence of liquid crystals is detected by observing the transmission of light when a cm-thick sample tube is observed that is enclosed between crossed polarizers.

The phase diagram is strongly influenced by the nature of the diluent. We have chosen four examples:

- iso-octane, a diluent that mixes easily with HDEHP chains. This diluent belongs to the class of penetrating diluents used in lubrication for diluent-chain compatibility [64]. The diluent penetration is also known to inhibit the formation of lyotropic liquid crystals, thus allowing the intensification of liquid–liquid extraction processes.
- Toluene, due to its polarity, allows for greater solubilization of rare earths in the diluent-rich phase and a higher extractant content with good extraction/back-extraction properties.
- Dodecane as the “model” alkane is heavily used on an industrial scale since it has a significantly lower vapor pressure. Due to its long and relatively stiff nature, dodecane has poor penetration properties compared to toluene and iso-octane.
- A well-known hydrotrope used extensively in industry, 1-propoxy-2-propanol PnP [65,66]. Hydrotropes are known to facilitate the solubilization of insoluble species, which favors the presence of trivalent salts even in the diluent phase [67,68]. The first hydrotrope used in perfumery is ethanol, and its role in the solubilization of volatile fragrances, such as in “Eau de Cologne”. The PnP is one of the most used and studied of all hydrotropes in the formulation [69,70].

The availability of phase diagrams provides access to crucial knowledge: an efficient extraction needs to be performed in a Winsor II regime, where reversed micelles (L2) saturated with water are in equilibrium with an excess water phase. However, no phase triangle should exist nearby with a concentrated third phase that is most of the time a liquid crystal.

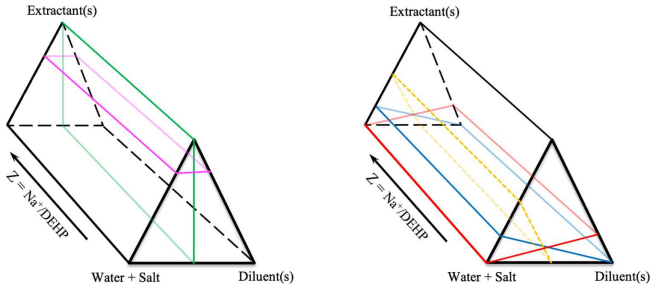

Fig. 1. In ternary and pseudo-ternary systems, the most natural representation is made from stacking phase triangles at a given temperature in the form of a prism, shown in black. In the case of extractants, the mole fraction of cation relative to anionic extractant (Z) governs spontaneous curvature and hence replaces the temperature as the edge of the prism. The figure shows on the left the two most used cuts in theoretical approaches that were introduced by Shinoda: the chi-cut (shown in magenta) and the "balanced" fish-cut (shown in green). On the right, the two cuts most used in chemical engineering to evaluate yields and safety of processes are shown: the Lund cut with constant water to extractant ratio (shown in red), the Lund cut with constant diluent to extractant ratio (shown in blue) and the formulator's cut at overall constant water content (shown in dashed orange lines).

Finally, phase prisms are useful to catch the global behavior but are difficult to read in detail when all triangles are stacked together in a 3D figure. In practice, three types of "cuts" of the phase prism are used, and their construction is shown in Figure 1 above.

The so-called "fish cut" – shown in green – highlights the domain of low effective curvature. It is useful when it is crucial to obtain large amounts of solutes with a small amount of extractant.

The "chi-cut" introduced by Shinoda [71] – shown in magenta – focuses on the water-rich to diluent-rich ternary solutions. Either continuous paths from the water-rich corner or a sudden phase separation with a meniscus are observed. The gradual transition is obtained for flexible microemulsions, while a discontinuous transition is observed in the case of rigid molecular films [5]. These two cuts presented on the right side of Figure 1 focus on the expected behavior at a fixed concentration of extractant in the solvent or water phase.

On the right part of Figure 1, three more cuts are presented. The "Lund-cut" is shown in red. This cut focuses on types of solutions that can be obtained with a fixed amount of extractant in the solvent phase. For water-soluble extractants, the Lund cut corresponds to the rectangle shown in blue. The Lund-cuts based on dilution with water (in red) or with a diluent (in blue) are useful to test proposed theories of conductivity, as well as scattering, and even for the validation of appropriate equations of state [72].

To optimize the amount of salts and acids to be used in a liquid–liquid extraction process, a peculiar cut, the "formulator's cut" has been proposed [73]. The formulator's cut is shown as an orange dashed line in the phase prism.

3 Experimental section

3.1 Substances

The diluents, toluene (purity > 99%), iso-octane (EA) (purity > 99.5%), dodecane (purity > 99%), ethanol (purity ≥ 99.9) and tert-butyl alcohol (purity > 99%) were purchased from Merck. Bis(2-ethylhexyl) phosphoric acid (purity > 97%) and 1-propoxy-2-propanol (purity > 99%) were purchased from Merck. Water was deionized using a Millipore Milli-Q purification system (Merck Millipore, Billerica, MA). All chemicals were used without further purification.

3.2 Preparation of NaDEHP

NaDEHP is a component that is not found in a regular portfolio of big companies providing chemical products for laboratory use, such as Sigma Aldrich, Merck, or Carlo Erba. Its acidic counterpart, however, bis(2-ethylhexyl) phosphoric acid, or HDEHP, is easily accessible at a low price as it is one of the most used extractants in a laboratory as well as on an industrial scale.

For the synthesis of sodium salt, several procedures have been identified in the literature, such as the reaction of HDEHP with metallic sodium [57] or neutralization with sodium hydroxide until a certain pH [53,55]. While the first description was discarded beforehand due to safety reasons, the reports on neutralization with a base are ambiguously described. In one case, the equivalent point was set at pH = 6 [55], in the second case at pH = 9 [53]. One of the reasons for the deviation of the neutralization point could be the different choice of solvent (e.g., methanol and n-heptane) in which HDEHP was solubilized before the addition of aqueous NaOH. From a practical point of view, the first essays have been made with either of the proposed pathways, however, the presence of water in higher quantities has posed severe problems during evaporation of the solvent. Due to the surfactant properties of NaDEHP as the solution exhibits a gel-like texture with strong foam formation as the solution is more and more reduced.

As a consequence of the elusive procedures in literature, a novel concept has been developed in order to synthesize NaDEHP at high quantities on a laboratory scale (∼30 g per batch), with high yields and purity, in addition to a concise pathway.

3.2.1 The chemical reaction and challenges towards an easy purification

As this is a simple acid-base reaction, water is produced as a side product. Further, being a phosphoric acid, HDEHP is considered a strong acid (pK_a = 1.8) [74] the balance of the reaction is quantitatively towards the formation of NaDEHP.

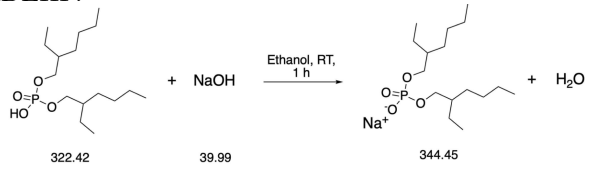

The crucial points of this reaction have been identified to be the addition of water and the volatility of the solvent. Therefore, a solvent has been chosen to commonly solubilize the reagents NaOH and HDEHP, which have been found in short-chained alcohols like methanol and ethanol. As an additional advantage, both alcohols form an azeotrope with water, thus facilitating the removal of water as a side-product of the reaction [75].

The second point is to ensure a complete reaction towards the salt, hence either the acid or the base needs to be added with slight excess. It was chosen to add NaOH in slight excess since after evaporation of the solvent after reaction, NaOH and NaDEHP remain as precipitates on the bottom of the flaks, and washing with water easily dissolves the base, while the salt remains solid. Finally, the overall reaction is depicted in the scheme above.

3.2.2 Working procedure

The first step is the solubilization of crushed sodium hydroxide pellets (1.05 eq, 91.45 mmol, 3.657 g) in ethanol (50 mL) in a flask (250 mL). To accelerate this process, the flask is put in an ultrasonic bath (20 min, RT). After obtaining a clear transparent solution, the flask is placed on a microbalance and HDEHP is added with a Pasteur pipette (1 eq, 87.1 mmol, 28.081 g). The solution is then stirred for 1 h at ambient conditions before evaporating the solvent under reduced pressure (180 mbar, 40 °C, 15 min) until white, waxy solid remains. Residual NaOH is removed by washing the product with water (3×20 mL). Water was removed by freeze-drying (12 h) to remove the major part, then under vacuum (24 h, 80 °C) to eliminate any residues. In the end, 29.6 g of pure NaDEHP was obtained (98.6% yield).

3.3 Preparation of phase diagrams

3.3.1 Experimental evaluation

The ternary phase diagrams have been evaluated by preparing 10 samples per dilution line at fixed Z. Samples have been prepared to start either from the water-extractant binary and diluted with diluent or the reverse (i.e., diluent-extractant binary and diluted with water).

The initial (pseudo-)binary compositions were chosen for fixed contents of extractant S_0^* that is always a mixture of NaDEHP and HDEHP at known Z and water W_0^* with:

$$S_0^* = \frac{w_{\text{extractant}}}{w_{\text{extractant}} + w_{\text{solvent}}}; W_0^* = \frac{w_{\text{extractant}}}{w_{\text{extractant}} + w_{\text{water}}}$$

with S_0^* or $W_0^* = 0.1, 0.25, 0.4, 0.55, 0.7$.

The initial sample mass before adding the last component was $m = 2$ g. All phase diagrams have been determined at ambient temperatures ($T = 25$ °C). The samples were prepared in closed tubes of borosilicate glass (from Pyrex).

Monophasic regions have been evaluated by diluting with the last component until a phase separation was observed by the naked eye (cloud-point method) [76]. The component used for the dilution lines was added in steps of 3–5 wt%, the solution was thoroughly shaken and left 24 h at constant temperature (25 °C) for settling. If no phase separation occurred within 48 h, the tubes were centrifuged for 30 min at 4500 rpm. The phase transitions were determined with the naked eye and through two cross-polarized filters in order to check the presence of liquid crystals. The amount of water or diluent added until the phase transition occurred was obtained with precise weight measurements. The weight fractions were then calculated for each formulation, and the pseudo-ternary phase diagram was built.

3.3.2 Plotting

The phase transitions have been plotted using the program Origin 8.5 from OriginLab. Interpolation of the phase transitions to give a phase boundary has been done using PowerPoint from Microsoft. The legend for the defined phases, which have been observed during this investigation, are:

- μE: monophasic region.
- 2: Biphasic liquid–liquid region.
- $[\mu E + I]_{2,3}$: multiple phases.
- $[\mu E + LC]_2$: lyotropic phases.
- $[\mu E + LC]_3$: 3 phases.
- S_h: Biphasic solid-liquid region.

3.3.3 Tie line analysis

The compositions of the quaternary solutions have been analyzed using different techniques in order to quantify a component in an organic or aqueous phase.

(i) Karl-Fischer analysis

The water-content in water-poor organic solutions has been determined by volumetric Karl-Fischer titration. An automated KF Titrando (Metrohm) device has been used, with a Composite 2 solution provided by Sigma Aldrich (2 mL of solutions are equivalent to 1 mg water).

(ii) Quantitative NMR

The content of toluene and the DEHP-anion has been determined using quantitative NMR with dimethylformamide as the internal standard, as it is soluble in water as well as in apolar solvents. Further, the chemical shift of the 1H spectrum can be clearly distinct from the signal of DEHP and toluene. NMR measurements have been carried out with a Bruker 400 device.

(iii) ICP-OES

The concentration of sodium in the aqueous and organic phase were analyzed by ICP-OES. The samples were analyzed by an ICP-OES spectrometer from Archos equipped with an autosampler. In order to avoid and notice cross-contamination, the system was rinsed with 2% (v/v) nitric acid, and blancs were placed at regular intervals.

(iv) Small angle X-ray scattering

Small-and-wide-angle X-ray scattering (SWAXS) measurements were performed on a bench built by XENOCS using Mo radiation ($l = 0.071$ nm). The scattered beam was recorded using a large online scanner detector (diameter: 345 mm, from MAR Research). A large q-range (0.2–40 nm^{-1}) was covered with an off-center detection. Collimation was applied using a 12:∞ multilayer Xenocs mirror (for Mo radiation) coupled with two sets of scatterless FORVIS slits providing a 0.8×0.8 mm X-ray beam at the sample position. Pre-analysis of data was performed using FIT2D software. The scattered intensities are recorded versus the magnitude of the scattering vector ($q = \left(\frac{4\pi}{\lambda}\right) \sin \frac{\theta}{2}$), where λ is the wavelength of incident radiation and θ the scattering angle. 2 mm quartz capillaries were used as sample containers for the solutions. The usual corrections for background (empty cell and detector noise) subtractions and intensity normalization using a high-density polyethylene film as a standard were applied. The experimental resolution was $\Delta q/q = 0.05$. Silver behenate in a sealed capillary was used as the scattering vector calibration standard. Measurements were performed at room temperature.

(v) Density maps

Solution densities were determined using a vibrating tube density meter (DMA 5000 M, Anton Paar, Austria) at (25 ± 0.005) °C with a nominal precision of $\pm 5 \times 10^{-6}$ g/mL. Calibration was performed using air and pure water at 25 °C. At the beginning and the end of each day, calibration was checked using pure water and between each measurement against air (maximum deviation: $\pm 5 \times 10^{-5}$ g/mL).

The end-points of the tie-lines when hydrotropes were used as a diluent were obtained through density measurements. Biphasic samples were prepared by mixing the first extractant and hydrotrope. After the addition of the residual amount of water, the solution was thoroughly mixed by hand. Subsequently, phase separation of the milky mixture was accelerated by gentle centrifugation (1500 g for 15 min) using a ROTINA 380 R centrifuge. The two phases obtained were carefully separated and collected in sealed vessels for density measurements. The determined densities were placed in the density map obtained before (see Fig. S1 in supplementary material) to deduce the composition of both water-rich and diluent-rich separated phases.

3.3.4 Critical point determination

In order to determine the position of the critical point in the system water/extractant/hydrotrope, different ternary mixtures were prepared within the clear and homogeneous (i.e., monophasic) region near the phase separation border in closable, volume-scaled tubes of borosilicate glass at room temperature. A fixed small amount of water and diluent was added very slowly to reach the phase boundary. After complete phase separation, the volume ratio between water- and diluent-rich phases was determined. The critical point corresponds to the extrapolation of the formulations, both having separated phases with equal volumes, to the phase boundary.

4 Results

In total, five phase diagrams in the pseudo ternary regime have been prepared for each diluent, alongside the two faces of the prism. An inconvenience of the pseudo- ternary representation is that the initial fixed ratio between the DEHP-derivatives may vary upon entering a multiphasic regime. As a consequence, no tie lines are represented in this section but are reviewed later.

4.1 Toluene used as the diluent

Figure 2 shows triangular sections of the phase prism obtained for different values of Z: $Z = 0$ corresponds to the pure HDEHP, where no sodium cation is present. The domain of water-poor reverse micelles is extremely small. All single phases connected to the toluene corner have been named μE for microemulsion, even if they are in physical terms more related to reverse micelles. Indeed, it is only at $Z > 0.8$ that more than 10 water molecules can be solubilized by H–NaDEHP: a complete inversion from w/o to o/w without phase separation occurs for NaDEHP/HDEHP: 80/20 ($Z > 0.8$).

The entire phase triangle at $Z = 0$ is occupied by a Winsor II equilibrium: a water-poor diluent phase at any concentration of HDEHP is easily contacted with excess water containing the ions to be extracted. The maximum amount of water per extractant in moles is less than two. Since there is no "free" water in the toluene-rich sample, this case is of little practical interest. If we turn to the $Z = 0.1$ or $Z = 0.3$ diagrams, we see that water uptake by the reverse micelle domain noted μE does not increase, while there is a risk of obtaining a spontaneous three-phase emulsion. This domain of composition corresponds to an aqueous isotropic phase but also to significant amounts of lyotropic liquid crystals, which form a spontaneous emulsion. Z-values below 0.50 are not suitable for liquid–liquid extraction. The situation is better for $Z > 0.7$, where only a small domain of instability containing a small amount of liquid crystal is detectable. Near this small domain of instability, the liquid probably exhibits some type of multi-layered microstructure. This has been reported in the case of water-soluble anionic surfactant and named L4 [77], as well as oil-soluble synthetic double-chain lipids recognized as a case of locally lamellar connected microemulsions [78–80].

The case of $Z = 0.9$ corresponds to the partition of the DEHP amphiphilic anion in the water-rich and the oil-rich-phases: this type of double aqueous biphasic system has been proposed for industrial use since the metals to be selectively extracted as well as the less hydrophilic extracting phases contain both more polar compounds than diluents [72].

Once all cations are replaced by sodium and the pure NaDEHP salt is used, Figure 2e, then $Z = 1$. This case

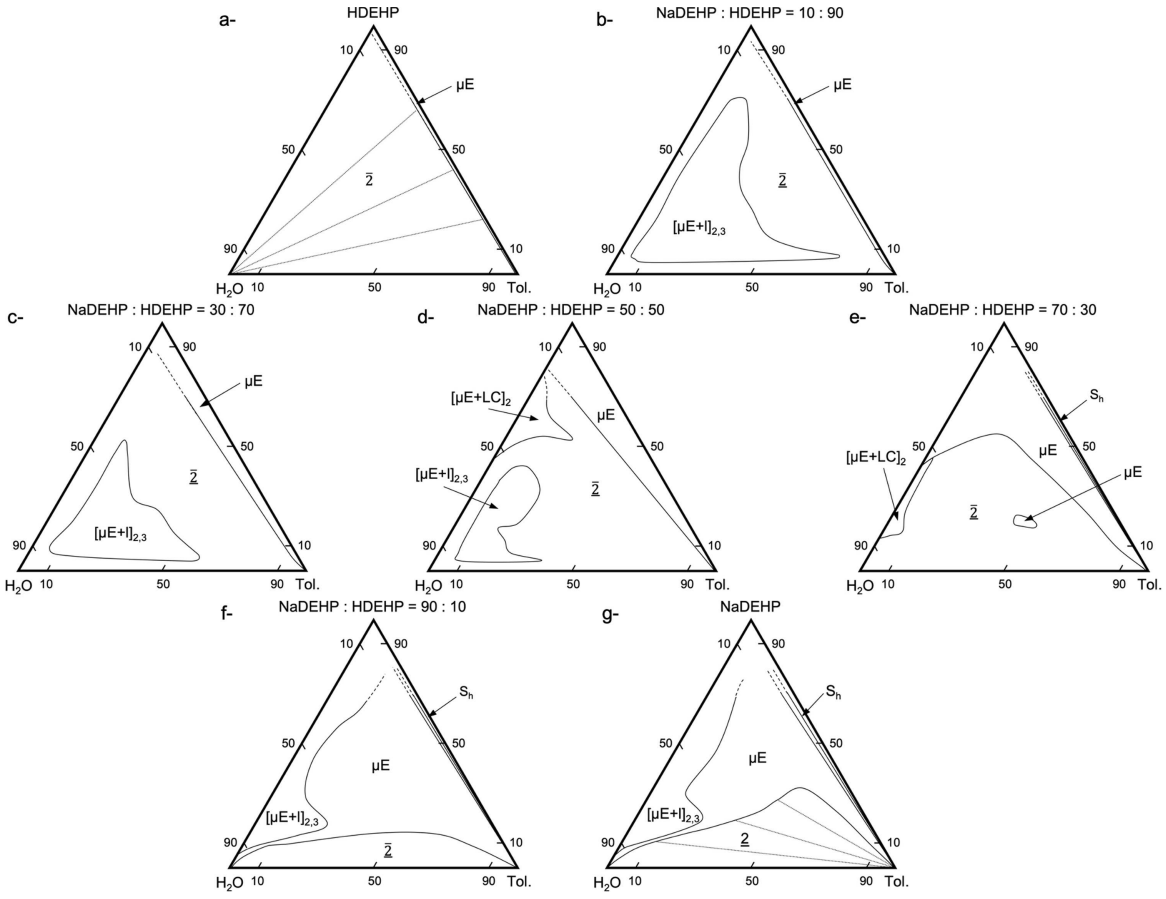

Fig. 2. Experimental pseudo-ternary phase diagrams of toluene/H–Na–DEHP/water in wt% for different ratios of H to Na. (a) $Z = 0$; (b) $Z = 0.1$; (c) $Z = 0.3$; (d) $Z = 0.5$; (e) $Z = 0.7$; (f) $Z = 0.9$; (g) $Z = 1$.

would be ideally suited for liquid–liquid extraction but only for oil-soluble components. This is used in pharmaceuticals and cosmetics, where the extraction of highly hydrophobic non-electrolytes is the goal. In addition, high acidities (pH $<$ 3) are a prerequisite condition for the extraction of trivalent cations such as lanthanides. Concentrated lanthanide solutions polymerize into gels that favor the formation of liquid crystals, so no hydrometallurgy can be performed in the range of Z close to 1. The location of the critical point is always on the toluene-rich side. At $Z = 0.9$, there is a very asymmetric phase transition [81].

In summary, Z-values below 0.1 avoid liquid crystals and provide safe Winsor II domains, useful for hydrometallurgical separation. However, the limited amount of water in the reverse micelles formed would be inadequate for the extraction of kosmotropic ions that induce high co-extraction of water extracted [82]. Selective extraction from chaotropic ions from mixtures containing chaotropic as well as kosmotropic mixtures can be performed in this range [82,83]. For $0.3 < Z < 0.6$, liquid crystals are present, so the third phase formation is possible. At high sodium content (Z close to 0.9), two-aqueous-phase extraction is possible. For pure HDEHP, there is an excess oil and a Winsor I equilibrium unsuitable for hydrometallurgical extraction.

4.2 Isooctane used as the diluent

Figure 3 shows the same triangular sections of the phase prism as the ones in Figure 2, this time using iso-octane instead of toluene. Iso-octane is branched in a way similar to the ethylhexyl branching of HDEHP. The mixing or "wetting" of the extractant and diluent chains is optimized. It has been shown that in this case, the penetration of the interdigitated diluent between chains of extractant decreases the spontaneous packing and decreases the polar cores of the reverse micelle formed [62,64,84].

A closer look at Figure 3 and comparison with Figure 2 shows that the global behavior is somewhat similar between toluene and iso-octane. The most important difference is that in the case of iso-octane, water is required to form reverse micelles from $Z > 0.5$, and they do not form in the absence of water. In addition, at $Z > 0.7$, solid extractant does not dissolve in the micellar solution, and a two-phase region is present near the binary axis extractant/iso-octane. Neumann et al. have shown that $w = 1$ is obtained for NaDEHP when heptane as a diluent is left in contact with the atmosphere at 50% humidity. Moreover, small micelles are more easily formed in the absence of water, as obtained with a strong drying agent in a glove box [85]. This solid region has also been observed in the case of AOT [26]. In the case of HDEHP, as well

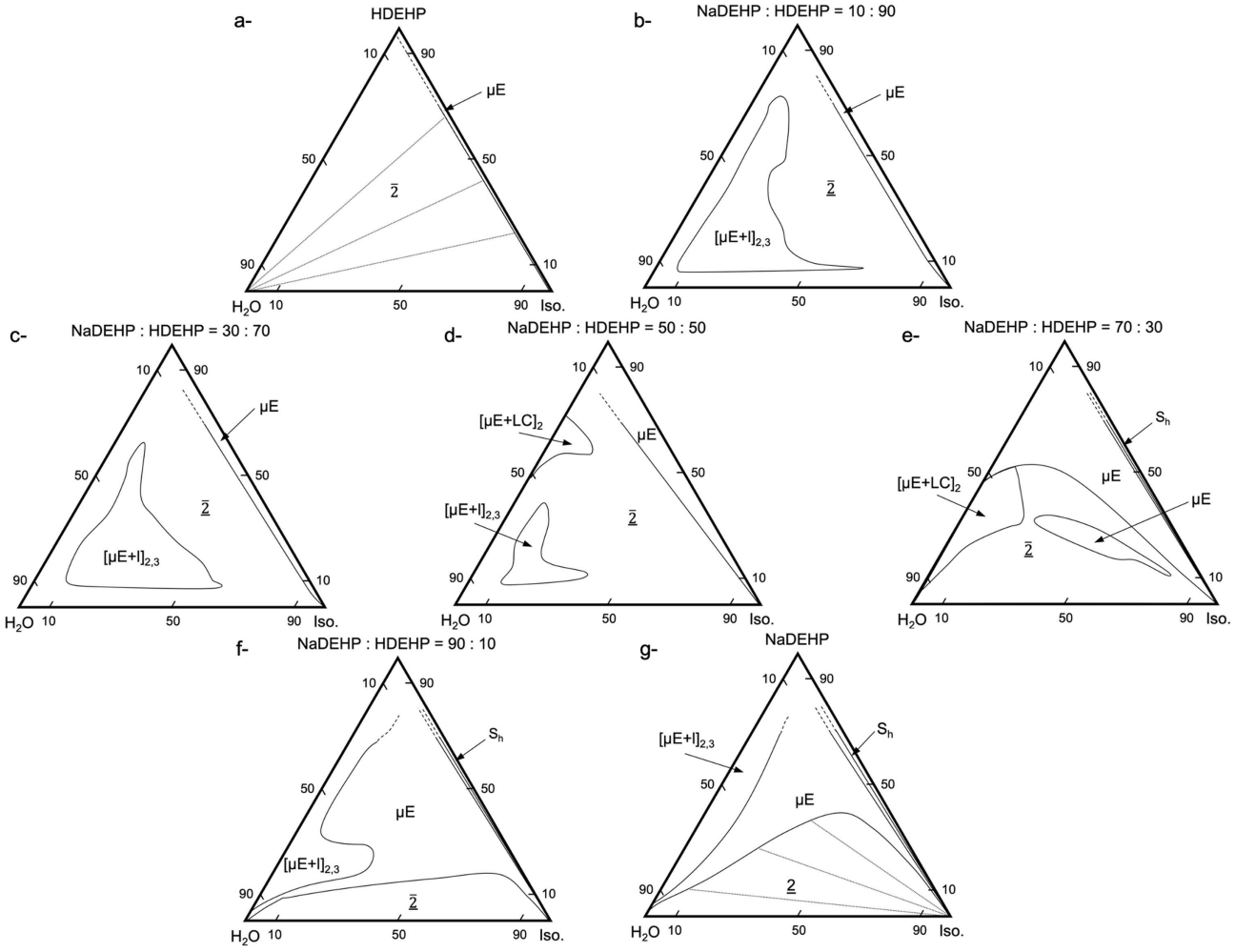

Fig. 3. Experimental pseudo-ternary phase diagrams of iso-octane/H–Na–DEHP/water in wt% for different ratios of H to Na. (a) $Z = 0$; (b) $Z = 0.1$; (c) $Z = 0.3$; (d) $Z = 0.5$; (e) $Z = 0.7$; (f) $Z = 0.9$; (g) $Z = 1$.

as AOT, reverse micelles, or even weak aggregates do not seem to exist in the absence of water ($W_0 < 1$). Close to $Z = 0.5$, a fair amount of water can be extracted (15%). However, at ($Z = 0.5$), the presence of liquid water limits the extractant "loading" to 20% in iso-octane as a diluent. This choice of Z close to 0.5 and an extractant content lower than 20% may still be a good choice for hydrometallurgical processes. The location of the critical point is still similar to the case of toluene. Finally, close to $Z = 0.8$, tie-lines are almost horizontal in the miscibility gap: the fluctuation is between water and oil at constant extractant content. This is a condition for efficient transfer of ions when considered in its entirety and not restricted to supramolecular complexation only [12].

4.3 Dodecane used as the diluent

If we turn now to the phase triangles as established for the linear alkane dodecane, we see that they become complex and liquid crystals are present everywhere. For $0.7 < Z < 0.9$, three-phase regions with excess diluent, liquid crystals, and an o/w microemulsion coexist. This regime may be very useful for the delivery of pharmaceuticals in the form of hexasomes, but it is totally unsuitable for hydrometallurgy. The separation plant in La Hague, for example, uses branched diluents which are mixtures of molecules with different wetting properties, whereas some pilot plants in Japan started with linear alkanes. Using linear alkanes, metal loading can never be brought to the same values in the process designed as using mixtures of branched alkanes. The extraction yield is, therefore, lower since all liquid crystal domains need to be avoided (Fig. 4).

The difference between the ternary phase diagram of AOT [28,30] and HDEHP is striking. The spontaneous packing parameter p_0 of AOT is close to one in iso-octane and exactly equal to one in the presence of 0.5% NaCl at 40 °C [28,30], while the p_0 of HDEHP is higher than 3 and can be slightly higher than one for $Z > 0.9$. The spontaneous packing parameter p_0 is used to quantify the preferred geometry of a surfactant (or extractant) and the linked form of the interface. It depends on the chain length, the apolar volume, and the area per head-group of the considered surfactant (or extractant).

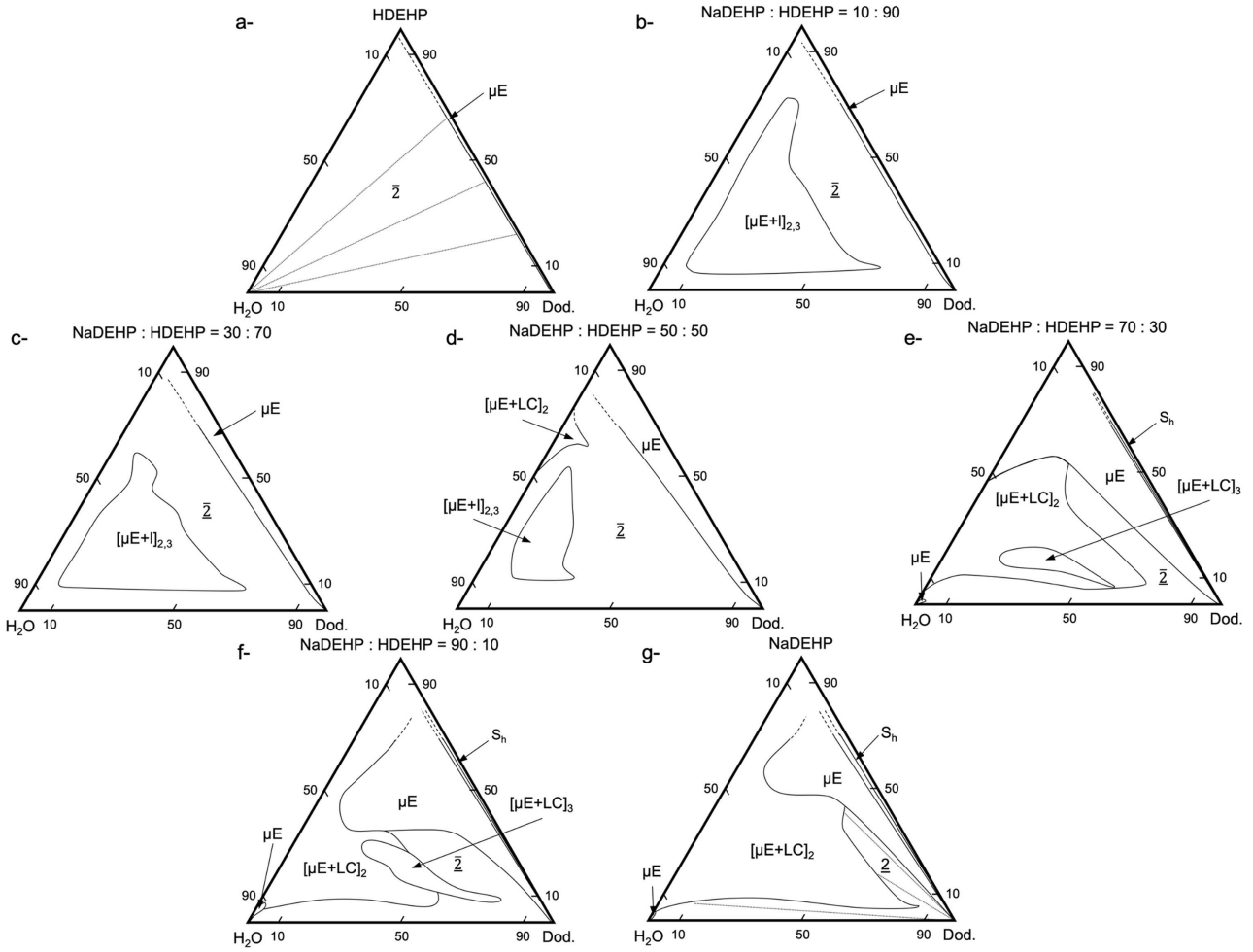

Fig. 4. Experimental pseudo-ternary phase diagrams of dodecane/H–Na–DEHP/water in wt% for different ratios of H to Na. (a) $Z = 0$; (b) $Z = 0.1$; (c) $Z = 0.3$; (d) $Z = 0.5$; (e) $Z = 0.7$; (f) $Z = 0.9$; (g) $Z = 1$.

In the case of pure HDEHP ($Z = 0$), it is not possible to adjust p_0 to be equal to one, as the head group is too small to compensate for the two branched chains. However, the variation in the miscibility gap is similar when switching from penetrating toluene or iso-octane to non-penetrating alkanes (i.e., dodecane). As a result, AOT is strongly used for peptide and protein extraction, whereas HDEHP is suited for divalent or trivalent salt extraction since the phosphorus head-group induces complexation that is absent with AOT. Moreover, in the case of HDEHP, configurational entropy competing with complexation is dominant, while for AOT, the curvature frustration is dominant in the free energy of extraction [60,61,86,87].

4.4 PnP used as the diluent

A completely different strategy is to use hydrotropes instead of the diluent in liquid–liquid extraction. The use of hydrotropes instead of classical diluents started when ethanol extraction was preferred to extraction by hexane for pharmaceutical applications. Hydrotropes are known to quench any emergence of liquid crystals in the ternary phase diagrams, but they are miscible with water. The corresponding strategy was therefore named "Aqueous Biphasic System" (ABS). However, the knowledge of the complete phase diagram and the location of the tie-lines in the phase diagrams is the prerequisite for the safe development of aqueous biphasic systems. Since they both contain significant amounts of water molecules, large variations in coacervation phenomena must be avoided when the cations to be separated are added [88].

Table 1 shows the properties of some common hydrotropes. Ethanol has been the most used hydrotrope in perfumery since the first development of Eau de Cologne. Moreover, back-extraction is simply made by evaporation of the volatile ethanol [89]. Due to their high flash point, the most suitable uncharged hydrotropes are propylene glycol propyl ether (PnP) and di(propylene glycol) propyl ether (DPnP). Hydrotropes have sometimes been considered close to short-chain amphiphiles: however binary solutions of hydrotropes in water or in classical diluents do not form micellar aggregates by themselves [67,90].

Table 1. Some properties of common hydrotropes.

Hydrotrope	Solubility in water g/L	Molar mass (g/mol)	Density at 25 °C (g/cm^3)	Refractive index (25 °C)	Melting temperature (Tf) (°C)	Boiling temperature (°C)	Flash point (°C)	Saturating vapor pressure at 20 °C (mbar)	CAS registry number
Ethanol	Miscible	46.0684	0.790–0.793	1.3594	−114.4	79	12	59	64-17-5
Aceton	Miscible	58.08	0.791	1.359	−94.6	56.05	−18	228	67-64-1
TBA	Miscible	74.1216	0.81	1.399	23–26	83	11	36	75-65-0
Isopropanol	Miscible	60.09	0.785	1.37723	−88.9	82.5	11.85	4.4 kPa	67-63-0
Isobutanol	87	74.1216	0.801	1.396	−108	108	28	40	78-83-1
Sec-butanol (butan-2-ol)	125	74.1216	0.8	1.3953	−115	100	24	1.7 kPa	78-92-2
Propylene glycol propyl ether (PnP): C_3PO_1	Miscible	118.17 118.17	0.885 0.885	1.411	−80 °C	140–160 140–160 140–160	48		1569-01-3
Urea	1080	60.055	0.750		132.7				57-13-6
di(propylene glycol) propyl ether (DPnP): C_3PO_2	19.6 (wt%)	176.25	0.92	1.424			88		29911-27-1
tri(propylene glycol) propyl ether C_3PO_3	14.4	234.33	0.935	1.43			113		96077-04-2

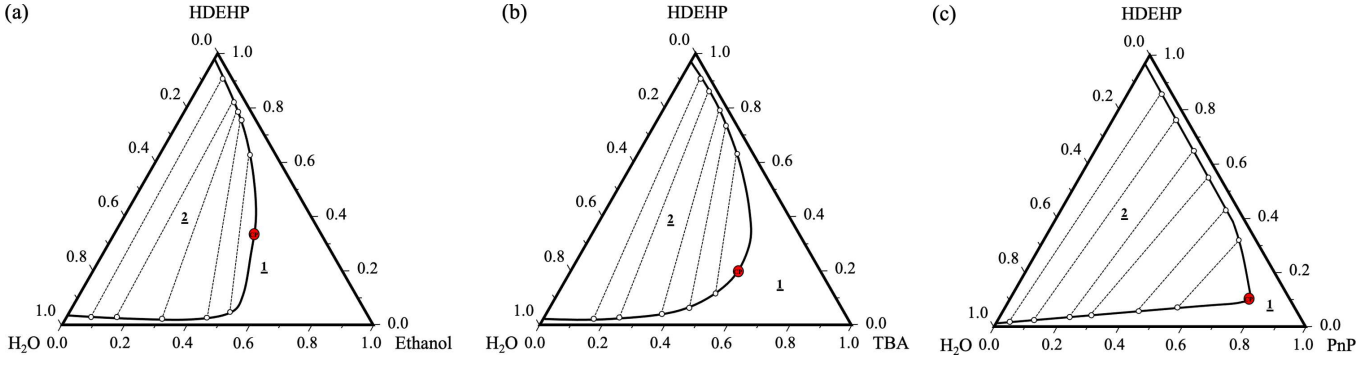

Fig. 5. Experimental ternary phase diagrams of hydrotrope/HDEHP/water in wt% for different hydrotrope: (a) ethanol (b) tert-butyl alcohol (c) PnP.

Figures 5a–5c show that three of the hydrotropes are not acting as real hydrotropes when the extractant HDEHP is considered a hydrophobic solvent. The water-HDEHP miscibility gap should be closed at values less than 40% in weight fraction in order to have a hydrotropic effect [91]. The miscibility gap is only closed at 50% of hydrotrope for ethanol and TBA, whereas 80% is necessary in order to obtain a monophasic phase in the case of PnP. Here, hydrotropes act as co-solvents of the water/HDEHP couple.

Figure 6 shows the dependence of the miscibility gap extension on the proportion of sodium counter-ion (i.e., Z). For NaDEHP (i.e., $Z = 1$), the hydrotropic effect starts, while in the range $0.2 < Z < 0.8$, the miscibility gap is close to 50%. In the case of ethanol, the binodal tie-lines open in a fan shape, while they are parallel to the water/HDEHP edge in the case of PnP. The critical point should be a common critical point since only the PnP concentration fluctuates between the two coexisting liquids. The critical point in ethanol is similar to the critical point in the binary system ethanol-dodecane [92].

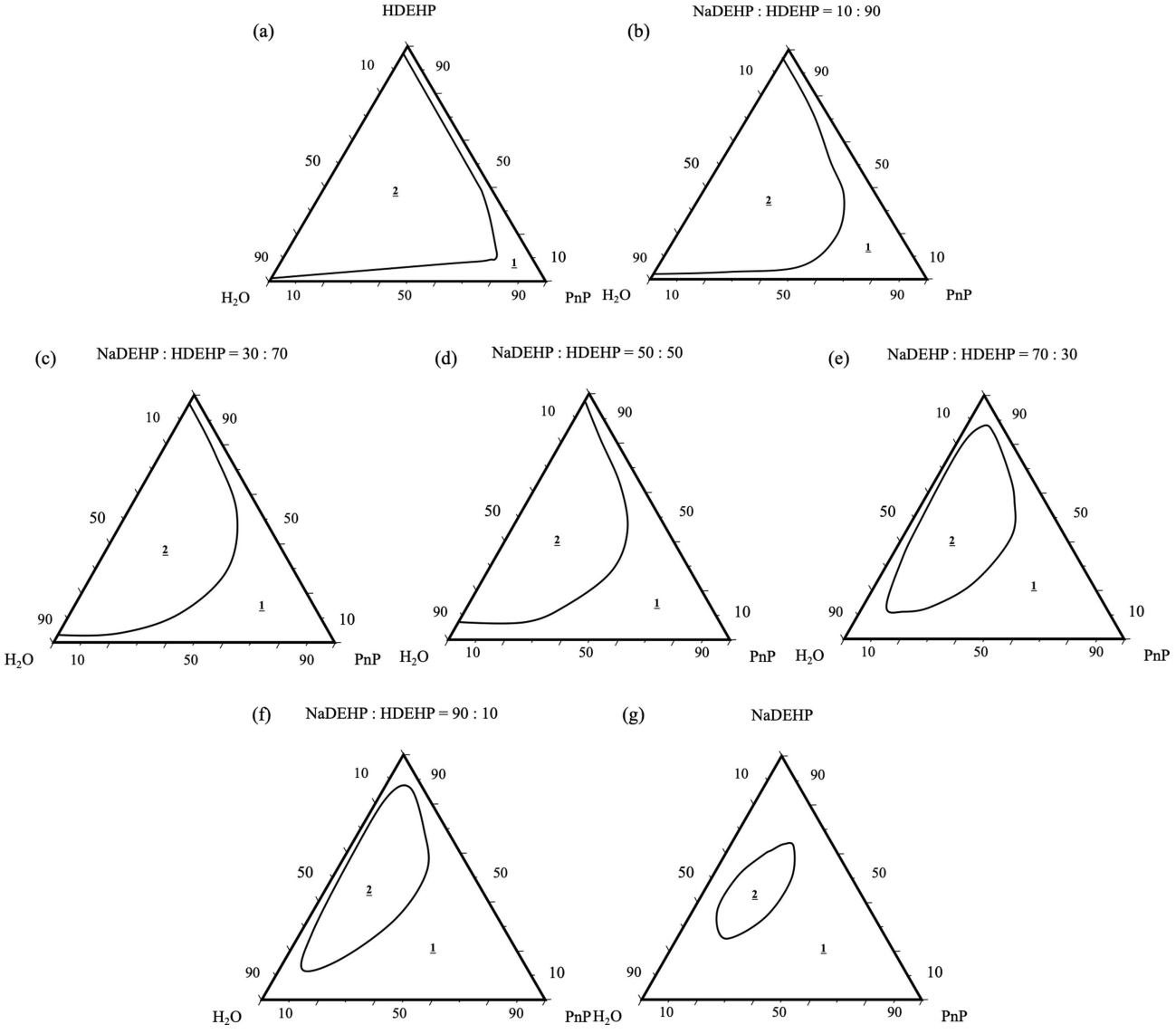

Fig. 6. Experimental pseudo-ternary phase diagrams of PnP/H–Na–DEHP/water in wt% and at room temperature for different ratios of H to Na. (a) $Z = 0$; (b) $Z = 0.1$; (c) $Z = 0.3$; (d) $Z = 0.5$; (e) $Z = 0.7$; (f) $Z = 0.9$; (g) $Z = 0.9$.

Note, however, that no liquid crystals exist: in the case of liquid–liquid phase separation performed in the miscibility gap, as expected from the general properties of hydrotropes, no liquid crystals are stable at any composition, even at room temperature. This property of hydrotropes is very convenient for designing safe chemical processes.

5 Discussion

The ternary phase diagrams, isolated or stacked along an axis that is spontaneous curvature, are useful for optimizing the formulations for liquid–liquid extraction. However, they are difficult to use for understanding the origin of the stability regions, two-phase equilibria, and the link with microstructure.

For these reasons, chi-cuts were introduced, using water to extractant mass ratio, as shown in Figure 7. The x-axis is now the polar weight fraction. On the left of the graph, the diluent is dominant, while to the right of the graph, water is dominant. The chi-cuts also contain information about sterically allowed microstructure. If we call s the area per extractant head-group (typically $0.6\,\mathrm{nm}^2$/molecule) [93–96], then the total available w/o interface per unit volume of samples is $s \times c_{\mathrm{ext}}$, with c_{ext} expressed in molecules per nm^3. When water is dominant, the radius of possible oily cores of o/w aggregates is $3 \times (1 - \Phi_{\mathrm{polar}})/\mathrm{s}$. with Φ_{polar} is the extractant polar volume fraction. When a diluent is a major component, similarly, the radius of possible w/o aggregates is $3 \times \Phi_{\mathrm{polar}}/\mathrm{s}$. As a first approximation, the sterically possible radii of dynamic aggregates should be compared to preferred radii related to the spontaneous packing of the extractant film:

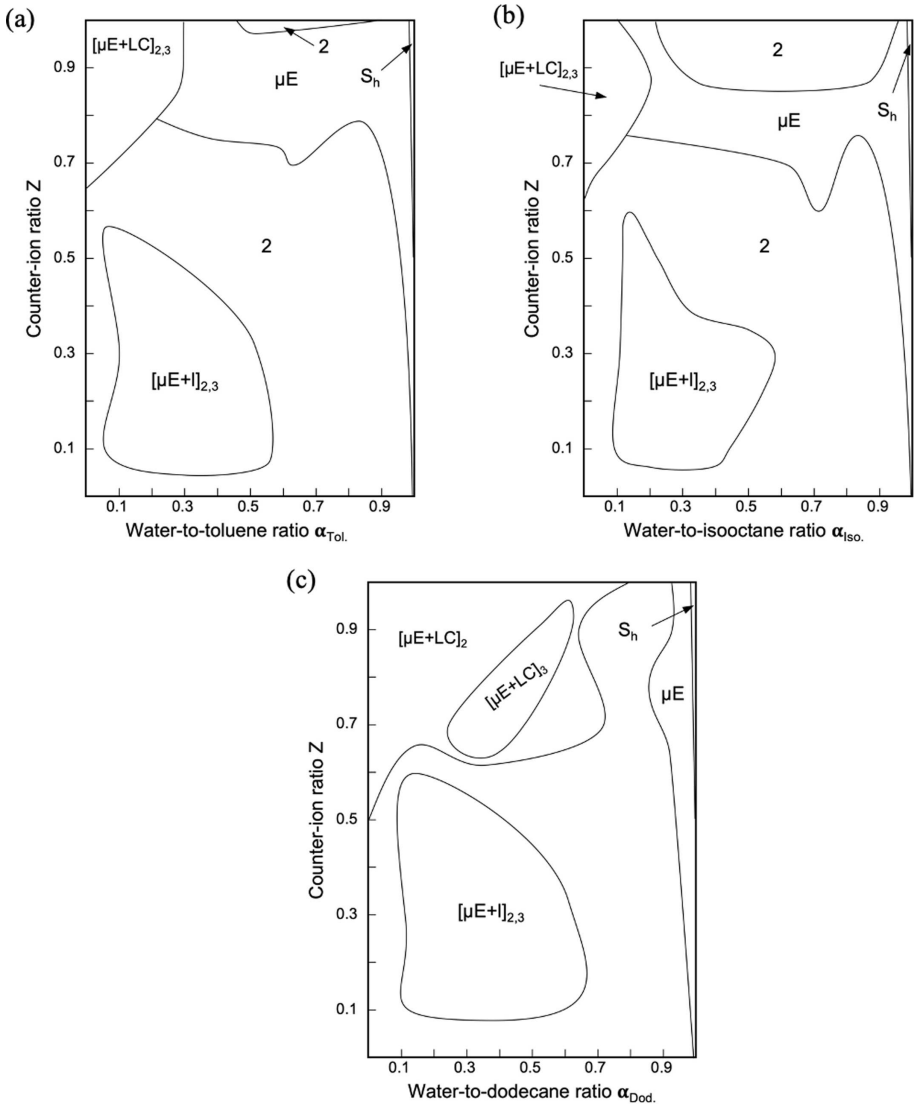

Fig. 7. Experimental chi-cuts of the phase prism using water-to-dodecane mass ratio as x-axis and the sodium counter-ion mol fraction Z controlling spontaneous curvature as y-axis. S_h is dry insoluble extractant, LC means one unidentified liquid crystal and μE refers either to a micellar solution or to a microemulsion. (a) Toluene (b) iso-octane (c) dodecane.

$r_0/l_{\text{ext}} = p_0 - 1$, where l_{ext} is the extractant chain length [97].

This simple argument allows a very straightforward interpretation of chi-cuts: when preferred radii correspond to possible radii, the micelles or microemulsions are stable, and when they differ, the packing is frustrated, and consequently, the free energy of the system is high. In chi-cuts, the monophasic domain limit resembles the greek-letter χ, hence the name of chi-cuts. Frustrated and non-frustrated regions can easily be detected by examining the chi-cuts. This has been shown initially with linear non-ionic ethoxylates [98] but also applies to extractants such as AOT [99].

If we now examine Figure 7 with this idea in mind that stable, non-frustrated w/o aggregates exist for low Z-values and high oil content at the bottom left of the graph, while o/w aggregates located at the top right are stable only using iso-octane. In the case of dodecane as well as toluene, in this region, liquid crystals are formed, making liquid–liquid extraction impossible. Further, the region for which the Winsor-II equilibria required for conventional liquid–liquid extraction exist is restricted to Z-values below 0.1. This limits the amount of metal to

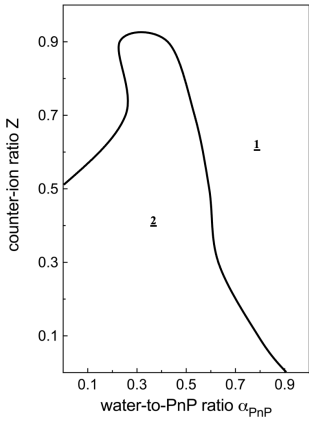

Fig. 8. Experimental chi-cut in the case of PnP, using HDEHP as extractant, and PnP as co-solvent.

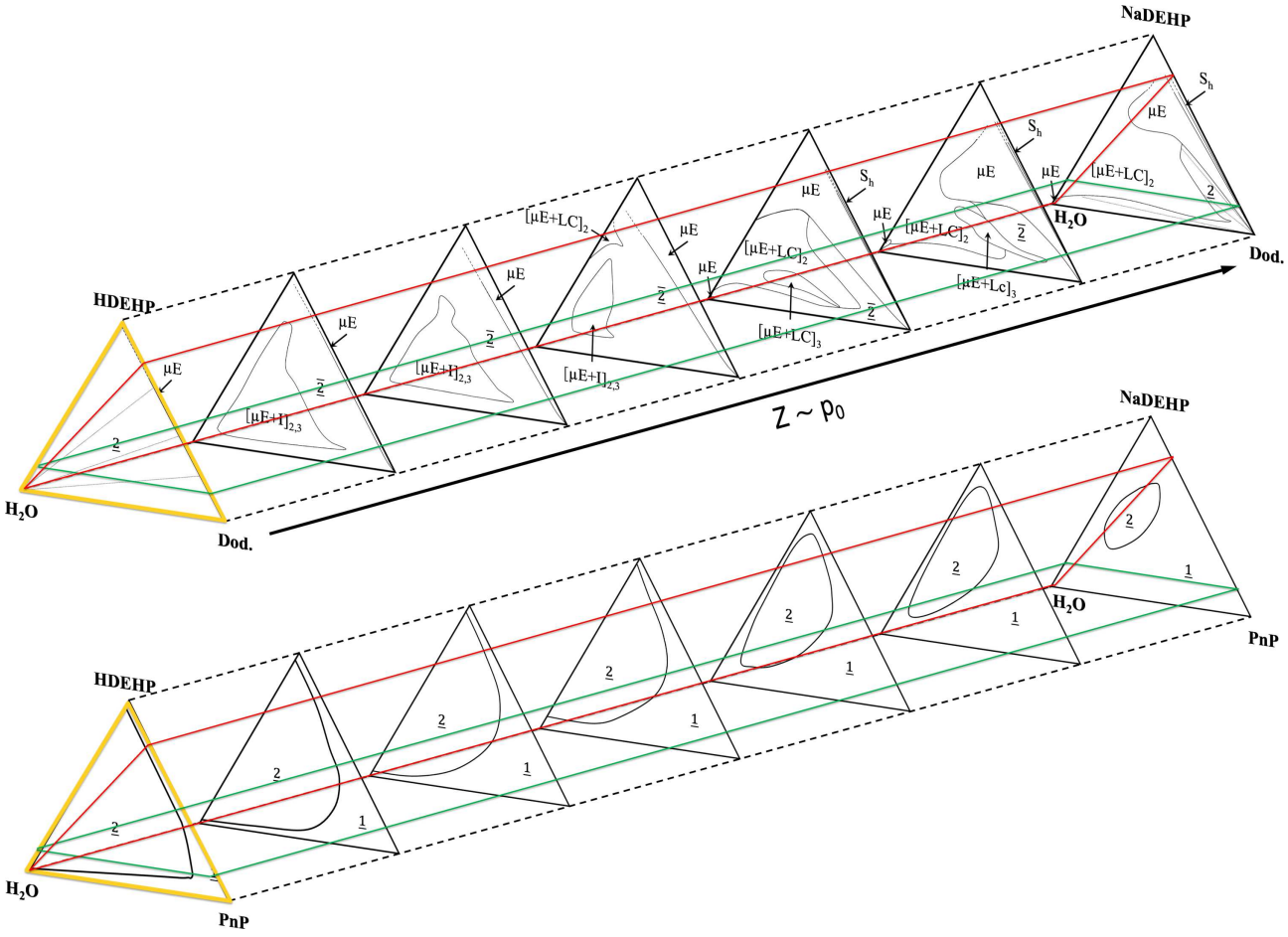

Fig. 9. The complex phase prism with a classical diluent (toluene) on the top versus a much simpler one with a co-solvent that is safer for extractions (PnP) on the bottom.

be extracted to extractant present between 3 and 5%. The intensification of the processes using these diluents requires adding "lipotropes" to the diluent-rich phase [13]. In the case of iso-octane as a diluent, a liquid–liquid miscibility gap exists close to $Z = 0.9$.

If we turn now to the chi-cuts made in the case of PnP, as shown in Figure 8, it is clear that there is neither a liquid crystal domain nor a third phase region and that liquid–liquid separation is possible at any value of Z. The two-phase domain is large. This property allows high molar ratios between the anionic extractant and the rare earths to be extracted, while designing intensified hydrometallurgical processes.

The main drawback is the perilous miscibility of the hydrotrope in the water-rich phase, like in all aqueous biphasic separation systems.

Finally, the Lund cuts are shown in their two forms in the Supplementary material (see Figs. S3a–S3d and S4a–S4d). These cuts are useful for checking the predictive power of free energy expression in the form of an equation of state [72]. Currently, only two types of equations of state allow one to approximately predict the phase diagram. This is only the case when considering monodisperse spherical droplets [100,101] or an extremely thin surfactant film, according to the Helfrich approximation [102]. The Lund cut for the hydrotrope studied (PnP) shows a monophasic domain increase with Z, the instability is the nucleation of water droplets. This would be an inverse Ouzo effect that has only been mentioned briefly in the seminal work about the Ouzo effect by Vitale and Katz [103]. We hope that this work will trigger further research and development of thermodynamic theory about w/o microemulsions, with quantitative predictions on Winsor II equilibria, far from any liquid crystal.

6 Conclusion

This study of the dependence of the phase diagram on the diluents highlights the importance of a proper choice of diluent in the search for more innovative, efficient, and eco-friendly liquid–liquid extraction. Process intensification and effluent reduction are possible to conceive by using systems with appropriate tie-lines in the phase prism. Figure 9 compares the two situations: hydrotropes used as co-solvents have the property of being safe regarding liquid crystal formation while allowing larger domains

of Winsor-II equilibria that can be exploited in liquid–liquid extraction. While efforts to improve liquid–liquid extraction have been made by systematic testing so far, in the future, advances in efficiency will be made by establishing phase diagrams and determining the corresponding transfer of free energy [35,104].

The main missing point today is the development of a predictive theory of phase stability via the relevant equation of state established from a parameter-free expression of free energy for extractant-based micelles and microemulsion. Predictive modeling of the Lund-cuts, as shown in the appendix, has been made successfully for the first time for the ternary system water–heptane–hexadecyl hexaethylene oxide ($C_{16}E_6$) by Ishikawa and co-workers [102]. We, therefore, hope that the availability of an increasing number of phase diagrams will trigger the development of predictive theories taking into account not only short-range interactions such as complexation but also solvent organization (entropy), at least in the first nanometre around any cation [105].

Acknowledgements

This research was done via two special "thèse-phare" PhD grants granted to CEA/DRF by the High-commissar of eatmoic energy. The PhD of Tobias Lopian was in co-responsability between the University of Montpellier and the University of Regensburg after initial support from the Master programm "COSOM".

Conflict of interests

The authors declare that they have no competing interests to report.

Funding

This work has been made due thanks a special funding "thèse phare amont-aval" attributed by Yves Brechet, High commissar of CEA. The SANS was performed via the fast test access at ILL D11 ILL AGA EASY-887.

Data availability statement

The data from neutron scattering can be found at DOI: 10.5291/ILL-DATA.EASY-887. This article has no SAXSassociated data generated and/or analyzed then the one found in figures and in the SM section.

Author contribution statement

Asmae El Maangar and Tobias Lopian performed the phase diagram determination. Sandrine Dourdain, Werner Kunz and Thomas Zemb designed the experiment and cross-checked the experimental results the experiment. Asmae El Mangar, Werner Kunz and Thomas Zemb wrote the final manuscript.

Supplementary Material

Lund cuts shown in their two forms. The Supplementary material is available at https://www.epj-n.org/10.1051/epjn/2022025/olm.

References

1. E. Paatero, J. Sjöblom, Phase behaviour in metal extraction systems, Hydrometallurgy **25**, 231 (1990)
2. R.G. Laughlin, *The Aqueous Phase Behavior of Surfactants*, 1. print. pbk. edition (Academic Press, London, 1996)
3. T. Zemb, W. Kunz, Weak aggregation: state of the art, expectations and open questions, Curr. Opin. Colloid Interface Sci. **22**, 113 (2016)
4. Y. Chevalier, T. Zemb, The structure of micelles and microemulsions, Rep. Prog. Phys. **53**, 279 (1990)
5. M. Gradzielski, M. Duvail, P.M. de Molina, M. Simon, Y. Talmon, T. Zemb, Using microemulsions: formulation based on knowledge of their mesostructure, Chem. Rev. **121**, 5671 (2021)
6. K. Fontell, A. Ceglie, B. Lindman, B. Ninham, C.J. Nielsen, F. Urso, J. Weidlein, R.A. Zingaro, Some observations on phase diagrams and structure in binary and ternary systems of didodecyldimethylammonium Bromide, Acta Chem. Scand. A **40**, 247 (1986)
7. D. Roux, A.M. Bellocq, M.S. Leblanc, An interpretation of the phase diagrams of microemulsions, Chem. Phys. Lett. **94**, 156 (1983)
8. V.A. Parsegian, T. Zemb, Hydration forces: observations, explanations, expectations, questions, Curr. Opin. Colloid Interface Sci. **16**, 618 (2011)
9. J.-F. Dufrêche, T. Zemb, Bending: from thin interfaces to molecular films in microemulsions, Curr. Opin. Colloid Interface Sci. **49**, 133 (2020)
10. P.A. Winsor, Hydrotropy, solubilisation and related emulsification processes, Trans. Faraday Soc. **44**, 376 (1948)
11. T. Zemb, C. Bauer, P. Bauduin, L. Belloni, C. Déjugnat, O. Diat, V. Dubois, J.-F. Dufrêche, S. Dourdain, M. Duvail, C. Larpent, F. Testard, S. Pellet-Rostaing, Recycling metals by controlled transfer of ionic species between complex fluids: en route to "Ienaics", Colloid Polym. Sci. **293**, 1 (2015)
12. M. Špadina, J.-F. Dufrêche, S. Pellet-Rostaing, S. Marčelja, T. Zemb, Molecular forces in liquid–liquid extraction, Langmuir **37**, 10637 (2021)
13. P. Bauduin, F. Testard, T. Zemb, Solubilization in alkanes by alcohols as reverse hydrotropes or "Lipotropes", J. Phys. Chem. B. **112**, 12354 (2008)
14. R.D. Rogers, A.H. Bond, C.B. Bauer, Metal ion separations in polyethylene glycol-based aqueous biphasic systems, Sep. Sci. Technol. **28**, 1091 (1993)
15. C. Larpent, A. Laplace, T. Zemb, Macrocyclic sugar-based surfactants: block molecules combining self-aggregation and complexation properties, Angew. Chem. Int. Ed. **43**, 3163 (2004)
16. M. Pleines, Ph.D. thesis, Thése de l'Université de Montpellier, 2018
17. J. Rydberg, M. Cox, C. Musikas, G.R. Choppin, *Solvent Extraction Principles and Practice, Revised and Expanded* (Taylor & Francis, 2004)
18. B. Bonin, B. Bouquin, M. Dozol, M. Lecomte, A. Vall'ee, in *Nuclear Fuels*, edited by J.-F. Parisot (CEA Saclay and Groupe Moniteur, Paris, 2009)
19. E. Abonneau, P. Baron, C. Berthon, L. Berthon, A. Beziat, I. Bisel, L. Bonin, E. Bosse, B. Boullis, J.C. Broudic, M.C. Charbonnel, N. Chauvin, C. Den Auwer, B. Dinh, J. Duhamet, J.M. Escleine, S. Grandjean, P. Guilbaud, D. Guillaneux, D. Guillaumont, C. Hill,

J. Lacquement, M. Masson, M. Miguirditchian, P. Moisy, M. Pelletier, A. Ravenet, C. Rostaing, V. Royet, A. Ruas, E. Simoni, C. Sorel, A. Vaudano, L. Venault, D. Warin, A. Zaetta, P. Pradel, B. Bonin, B. Bouquin, M. Dozol, M. Lecomte, A. Forestier, M. Beauvy, G. Berthoud, M. Defranceschi, G. Ducros, Y. Guerin, C. Latge, Y. Limoge, C. Madic, G. Santarini, J.M. Seiler, P. Sollogoob, E. Vernaz, F. Bazile, J.P. Parisot, P. Finot, J.F. Roberts, *Treatment and Recycling of Spent Nuclear Fuel Actinide Partitioning – Application to Waste Management* (CEA and Editions du Moniteur, France, 2008), http://inis.iaea.org/search/search.aspx?orig_q=RN:41047159

20. C. Bauer, P. Bauduin, J.F. Dufrêche, T. Zemb, O. Diat, Liquid/liquid metal extraction: phase diagram topology resulting from molecular interactions between extractant, ion, oil and water, Eur. Phys. J. Spec. Top. **213**, 225 (2012)
21. B. Goldschmidt, *L'Aventure atomique* (Fayard, 1962)
22. Q. Li, T. Li, J. Wu, Water solubilization capacity and conductance behaviors of AOT and NaDEHP systems in the presence of additives, Colloids Surf. A: Physicochem. Eng. Aspects **197**, 101 (2002)
23. S. Nave, J. Eastoe, J. Penfold, What is so special about Aerosol-OT? 1. Aqueous systems, Langmuir **16**, 8733 (2000)
24. S. Nave, J. Eastoe, R.K. Heenan, D. Steytler, I. Grillo, What is so special about Aerosol-OT? 2. Microemulsion systems, Langmuir **16**, 8741 (2000)
25. M.J. Hou, M. Kim, D.O. Shah, A light scattering study on the droplet size and interdroplet interaction in microemulsions of AOT–oil–water system, J. Colloid Interface Sci. **123**, 398 (1988)
26. H.-F. Eicke, H. Christen, Is water critical to the formation of micelles in apolar media? Helv. Chim. Acta **61**, 2258 (1978)
27. M. Sagisaka, T. Narumi, M. Niwase, S. Narita, A. Ohata, C. James, A. Yoshizawa, E. Taffin de Givenchy, F. Guittard, S. Alexander, J. Eastoe, Hyperbranched hydrocarbon surfactants give fluorocarbon-like low surface energies, Langmuir **30**, 6057 (2014)
28. H. Kunieda, K. Shinoda, Solution behavior of aerosol ot/water/oil system, J. Colloid Interface Sci. **70**, 577 (1979)
29. T. Assih, Evolution of the radius of the inverse micelles at high dilution in the AerosoI-OT/water/*n*-decane system, J. Colloid Interface Sci. **89**, 5 (1982)
30. H. Kunieda, K. Shinoda, Solution behavior and hydrophile-lipophile balance temperature in the aerosol OT-isooctane-brine system: correlation between microemulsions and ultralow interfacial tensions, J. Colloid Interface Sci. **75**, 601 (1980)
31. A. Artese, S. Dourdain, N. Felines, G. Arrachart, N. Boubals, P. Guilbaud, S. Pellet-Rostaing, Bifunctional amidophosphonate molecules for uranium extraction in nitrate acidic media, Solvent Extr. Ion Exch. **38**, 703 (2020)
32. W. Dembiński, T. Mioduski, Europium isotope separation in the HCl/HDEHP extraction system, J. Radioanal. Nucl. Chem. Lett. **199**, 159 (1995)
33. J. Rey, S. Atak, S. Dourdain, G. Arrachart, L. Berthon, S. Pellet-Rostaing, Synergistic extraction of rare earth elements from phosphoric acid medium using a mixture of surfactant AOT and DEHCNPB, Solvent Extr. Ion Exch. **35**, 321 (2017)
34. G.J. Lumetta, A.V. Gelis, J.C. Braley, J.C. Carter, J.W. Pittman, M.G. Warner, G.F. Vandegrift, The TRUSPEAK concept: combining CMPO and HDEHP for separating trivalent lanthanides from the transuranic elements, Solvent Extr. Ion Exch. **31**, 223 (2013)
35. A. El Maangar, J. Theisen, C. Penisson, T. Zemb, J.-C.P. Gabriel, A microfluidic study of synergic liquid–liquid extraction of rare earth elements, Phys. Chem. Chem. Phys. **22**, 5449 (2020)
36. D. Beltrami, A. Chagnes, M. Haddad, H. Laureano, H. Mokhtari, B. Courtaud, S. Jugé, G. Cote, Solvent extraction studies of uranium(VI) from phosphoric acid: Role of synergistic reagents in mixture with bis(2-ethylhexyl) phosphoric acid, Hydrometallurgy **144–145**, 207 (2014)
37. S. Dourdain, I. Hofmeister, O. Pecheur, J.-F. Dufrêche, R. Turgis, A. Leydier, J. Jestin, F. Testard, S. Pellet-Rostaing, T. Zemb, Synergism by coassembly at the origin of ion selectivity in liquid–liquid extraction, Langmuir **28**, 11319 (2012)
38. J. Rey, S. Dourdain, J.-F. Dufrêche, L. Berthon, J.M. Muller, S. Pellet-Rostaing, T. Zemb, Thermodynamic description of synergy in solvent extraction: I. Enthalpy of mixing at the origin of synergistic aggregation, Langmuir **32**, 13095 (2016)
39. J. Rey, M. Bley, J.-F. Dufrêche, S. Gourdin, S. Pellet-Rostaing, T. Zemb, S. Dourdain, Thermodynamic description of synergy in solvent extraction: II Thermodynamic balance of driving forces implied in synergistic extraction, Langmuir **33**, 13168 (2017)
40. H.-F. Eicke, Surfactants in nonpolar solvents, in *Micelles* (Springer, 1980), pp. 85–145
41. Q. Li, T. Li, J. Wu, Comparative study on the structure of reverse micelles. 2. FT-IR, ^{1}H NMR, and electrical conductance of H_2O/AOT/NaDEHP/*n*-Heptane systems, J. Phys. Chem. B. **104**, 9011 (2000)
42. T. Lopian, Ph.D. thesis, Thése de l'Université de Montpellier, 2017
43. J.-M. Aubry, J.F. Ontiveros, J.-L. Salager, V. Nardello-Rataj, Use of the normalized hydrophilic-lipophilic-deviation (HLDN) equation for determining the equivalent alkane carbon number (EACN) of oils and the preferred alkane carbon number (PACN) of nonionic surfactants by the fish-tail method (FTM), Adv. Colloid Interface Sci. **276**, 102099 (2020)
44. E.J. Acosta, The HLD–NAC equation of state for microemulsions formulated with nonionic alcohol ethoxylate and alkylphenol ethoxylate surfactants, Colloids Surf. A: Physicochem. Eng. Aspects **320**, 193 (2008)
45. E. Acosta, Engineering cosmetics using the Net-Average-Curvature (NAC) model, Curr. Opin. Colloid Interface Sci. **48**, 149 (2020)
46. E. Acosta, E. Szekeres, D.A. Sabatini, J.H. Harwell, Net-average curvature model for solubilization and supersolubilization in surfactant microemulsions, Langmuir **19**, 186 (2003)
47. S.K. Kiran, E.J. Acosta, Predicting the morphology and viscosity of microemulsions using the HLD-NAC Model, Ind. Eng. Chem. Res. **49**, 3424 (2010)
48. R. Leung, D.O. Shah, Solubilization and phase equilibria of water-in-oil microemulsions, J. Colloid Interface Sci. **120**, 320 (1987)
49. R. Leung, D.O. Shah, Solubilization and phase equilibria of water-in-oil microemulsions II, J. Colloid Interface Sci. **120**, 330 (1987)

50. E. Paatero, P. Ernola, J. Sjöblom, L. Hummel-stedt, Formation of microemulsion in solvent extraction systems containing Cyanex 272, in Proceedings of the International Solvent Extraction Conference (ISEC'88) (1988), p. 124
51. E. Paatero, T. Lantto, P. Ernola, The effect of trioctylphosphine oxide on phase and extraction equilibria in systems containing bis(2,4,4-trimethylpentyl) phosphinic acid, Solvent Extr. Ion Exch. **8**, 371 (1990)
52. Z.-J. Yu, R.D. Neuman, Reversed micellar solution-to-bicontinuous microemulsion transition in sodium bis (2-ethylhexyl) phosphate/*n*-heptane/water system, Langmuir **11**, 1081 (1995)
53. A. Shioi, M. Harada, K. Matsumoto, Phase equilibrium of sodium bis(2-ethylhexyl)phosphate/water/*n*-heptane/sodium chloride microemulsion, J. Phys. Chem. **95**, 7495 (1991)
54. A. Shioi, M. Harada, M. Tanabe, Static light scattering from oil-rich microemulsions containing polydispersed cylindrical aggregates in sodium bis(2-ethylhexyl) phosphate system, J. Phys. Chem. **99**, 4750 (1995)
55. A. Faure, A.M. Tistchenko, T. Zemb, C. Chachaty, Aggregation and dynamical behavior in sodium diethylhexyl phosphate/water/benzene inverted micelles, J. Phys. Chem. **89**, 3373 (1985)
56. Z.-J. Yu, R.D. Neuman, Giant rodlike reversed micelles formed by sodium bis(2-ethylhexyl) phosphate in *n*-heptane, Langmuir **10**, 2553 (1994)
57. Z.J. Yu, N.F. Zhou, R.D. Neuman, On the role of water in the formation of reversed micelles: an antimicellization agent, Langmuir **8**, 1885 (1992)
58. A. Faure, T. Ahlnas, A.M. Tistchenko, C. Chachaty, Surfactant conformation and solvent penetration in sodium di-2-ethylhexyl phosphate reversed micelles. A multinuclear relaxation study, J. Phys. Chem. **91**, 1827 (1987)
59. S.S. Quintana, R.D. Falcone, J.J. Silber, N.M. Correa, Comparison between two anionic reverse micelle interfaces: the role of water–surfactant interactions in interfacial properties, ChemPhysChem **13**, 115 (2012)
60. E.B. Leodidis, T.A. Hatton, Amino acids in AOT reversed micelles. 1. Determination of interfacial partition coefficients using the phase-transfer method, J. Phys. Chem. **94**, 6400 (1990)
61. E.B. Leodidis, T.A. Hatton, Amino acids in AOT reversed micelles. 2. The hydrophobic effect and hydrogen bonding as driving forces for interfacial solubilization, J. Phys. Chem. **94**, 6411 (1990)
62. L. Berthon, L. Martinet, F. Testard, C. Madic, T. Zemb, Solvent penetration and sterical stabilization of reverse aggregates based on the DIAMEX process extracting molecules: consequences for the third phase formation, Solvent Extr. Ion Exch. **25**, 545 (2007)
63. S. Alexander, J. Eastoe, A.M. Lord, F. Guittard, A.R. Barron, Branched hydrocarbon low surface energy materials for superhydrophobic nanoparticle derived surfaces, ACS Appl. Mater. Interfaces **8**, 660 (2016)
64. S.J. Chen, D.F. Evans, B.W. Ninham, D.J. Mitchell, F.D. Blum, S. Pickup, Curvature as a determinant of microstructure and microemulsions, J. Phys. Chem. **90**, 842 (1986)
65. P. Bauduin, D. Touraud, W. Kunz, Design of low-toxic and temperature-sensitive anionic microemulsions using short propyleneglycol alkyl ethers as cosurfactants, Langmuir **21**, 8138 (2005)
66. P. Bauduin, L. Wattebled, S. Schrödle, D. Touraud, W. Kunz, Temperature dependence of industrial propylene glycol alkyl ether/water mixtures, J. Mol. Liq. **115**, 23 (2004)
67. W. Kunz, K. Holmberg, T. Zemb, Hydrotropes, Curr. Opin. Colloid Interface Sci. **22**, 99 (2016)
68. J. Mehringer, E. Hofmann, D. Touraud, S. Koltzenburg, M. Kellermeier, W. Kunz, Salting-in and salting-out effects of short amphiphilic molecules: a balance between specific ion effects and hydrophobicity, Phys. Chem. Chem. Phys. **23**, 1381 (2021)
69. B. Ramsauer, R. Neueder, W. Kunz, Erratum to "Isobaric vapour–liquid equilibria of binary 1-propoxy-2-propanol mixtures with water and alcohols at reduced pressure" Fluid Phase Equilibria 272 (2008) 84–92, Fluid Phase Equilib. **277**, 162 (2009)
70. B. Ramsauer, M.M. Meier, R. Neueder, W. Kunz, Conductivity studies of tetrabutylammonium salts in 1-propoxy-2-propanol: ion-association in dilute solutions, Acta Chim. Slovenica **56**, 30 (2009)
71. T.F. Tadros, *Self-Organized Surfactant Structures* (Wiley, Somerset, 2011)
72. M.S. Leaver, U. Olsson, H. Wennerström, R. Strey, U. Würz, Phase behaviour and structure in a non-ionic surfactant–oil–water mixture, J. Chem. Soc., Faraday Trans. **91**, 4269 (1995)
73. T. Lopian, S. Dourdain, W. Kunz, T. Zemb, A formulator's cut of the phase prism for optimizing selective metal extraction, Colloids Surf. A: Physicochem. Eng. Aspects **557**, 2 (2018)
74. R.J. Ellis, T. Demars, G. Liu, J. Niklas, O.G. Poluektov, I.A. Shkrob, In the bottlebrush garden: the structural aspects of coordination polymer phases formed in lanthanide extraction with alkyl phosphoric acids, J. Phys. Chem. B **119**, 11910 (2015)
75. Dow Chemical Company, L.H. Horsley, W.S. Tamplin, eds., *Azeotropic Data* (American Chemical Society, Washington, 1952)
76. M. Clausse, L. Nicolas-Morgantini, A. Zradba, D. Tourand, *Microemulsion Systems* (Marcell Dekker, 1987)
77. G. Guerin, A.M. Bellocq, Effect of salt on the phase behavior of the ternary system water-pentanol-sodium dodecylsulfate, J. Phys. Chem. **92**, 2550 (1988)
78. S.J. Chen, D.F. Evans, B.W. Ninham, Properties and structure of three-component ionic microemulsions, J. Phys. Chem. **88**, 1631 (1984)
79. F.D. Blum, S. Pickup, B. Ninham, S.J. Chen, D.F. Evans, Structure and dynamics in three-component microemulsions, J. Phys. Chem. **89**, 711 (1985)
80. I.S. Barnes, P.-J. Derian, S.T. Hyde, B.W. Ninham, T.N. Zemb, A disordered lamellar structure in the isotropic phase of a ternary double-chain surfactant system, J. Phys. France **51**, 2605 (1990)
81. J.J. Booth, S. Abbott, S. Shimizu, Mechanism of hydrophobic drug solubilization by small molecule hydrotropes, J. Phys. Chem. B **116**, 14915 (2012)
82. C. Déjugnat, L. Berthon, V. Dubois, Y. Meridiano, S. Dourdain, D. Guillaumont, S. Pellet-Rostaing, T. Zemb, Liquid-liquid extraction of acids and water by a malonamide: i-anion specific effects on the polar core microstructure of the aggregated malonamide, Solvent Extr. Ion Exch. **32**, 601 (2014)
83. C. Déjugnat, J.-F. Dufrêche, T. Zemb, Ion-specific weak adsorption of salts and water/octanol transfer free energy

of a model amphiphilic hexapeptide, Phys. Chem. Chem. Phys. **13**, 6914 (2011)
84. H. Kellay, B.P. Binks, Y. Hendrikx, L.T. Lee, J. Meunier, Properties of surfactant monolayers in relation to microemulsion phase behaviour, Adv. Colloid Interface Sci. **49**, 85 (1994)
85. Z.-J. Yu, N.-F. Zhou, R.D. Neuman, The role of water in the formation of reversed micelles: an antimicellization agent, Langmuir **8**, 1885 (1992)
86. E.B. Leodidis, A.S. Bommarius, T.A. Hatton, Amino acids in reversed micelles. 3. Dependence of the interfacial partition coefficient on excess phase salinity and interfacial curvature, J. Phys. Chem. **95**, 5943 (1991)
87. E.B. Leodidis, T.A. Hatton, Amino acids in reversed micelles. 4. Amino acids as cosfurfactants, J. Phys. Chem. **95**, 5957 (1991)
88. Y. Akama, Extraction mechanism of Cr(VI) on the aqueous two-phase system of tetrabutylammonium bromide and (NH4)2SO4 mixture, Talanta **57**, 681 (2002)
89. V. Tchakalova, T. Zemb, D. Benczédi, Evaporation triggered self-assembly in aqueous Fragrance–Ethanol mixtures and its impact on fragrance performance, Colloids Surf. A: Physicochem. Eng. Aspects **460**, 414 (2014)
90. S. Schöttl, D. Horinek, Aggregation in detergent-free ternary mixtures with microemulsion-like properties, Curr. Opin. Colloid Interface Sci. **22**, 8 (2016)
91. T.N. Zemb, M. Klossek, T. Lopian, J. Marcus, S. Schöettl, D. Horinek, S.F. Prevost, D. Touraud, O. Diat, S. Marčelja, W. Kunz, How to explain microemulsions formed by solvent mixtures without conventional surfactants, Proc. Nat. Acad. Sci. **113**, 4260 (2016)
92. T. Zemb, R. Rosenberg, S. Marčelja, D. Haffke, J.-F. Dufrêche, W. Kunz, D. Horinek, H. Cölfen, Phase separation of binary mixtures induced by soft centrifugal fields, Phys. Chem. Chem. Phys. **23**, 8261 (2021)
93. P. Bauduin, T. Zemb, Perpendicular and lateral equations of state in layered systems of amphiphiles, Curr. Opin. Colloid Interface Sci. **19**, 9 (2014)
94. Th. Zemb, L. Belloni, M. Dubois, A. Aroti, E. Leontidis, Can we use area per surfactant as a quantitative test model of specific ion effects? Curr. Opin. Colloid Interface Sci. **9**, 74 (2004)
95. C. Tanford, Micelle shape and size, J. Phys. Chem. **76**, 3020 (1972)
96. A. Aroti, E. Leontidis, M. Dubois, T. Zemb, Effects of monovalent anions of the hofmeister series on DPPC lipid bilayers Part I: swelling and in-plane equations of state, Biophys. J. **93**, 1580 (2007)
97. W. Kunz, F. Testard, T. Zemb, Correspondence between curvature, packing parameter, and hydrophilic-lipophilic deviation scales around the phase-inversion temperature, Langmuir **25**, 112 (2009)
98. S.-H. Chen, S.-L. Chang, R. Strey, Structural evolution within the one-phase region of a three-component microemulsion system: Water–*n*-decane–sodium-bis-ethylhexylsulfosuccinate (AOT), J. Chem. Phys. **93**, 1907 (1990)
99. L.J. Magid, K.A. Daus, P.D. Butler, R.B. Quincy, Aggregation of sulfosuccinate surfactants in water, J. Phys. Chem. **87**, 5472 (1983)
100. R.-N. Hwan, C.A. Miller, T. Fort, Determination of microemulsion phase continuity and drop size by ultracentrifugation, J. Colloid Interface Sci. **68**, 221 (1979)
101. M. Dvolaitzky, M. Guyot, M. Lagües, J.P. Le Pesant, R. Ober, C. Sauterey, C. Taupin, A structural description of liquid particle dispersions: ultracentrifugation and small angle neutron scattering studies of microemulsions, J. Chem. Phys. **69**, 3279 (1978)
102. K. Ishikawa, M. Behrens, S. Eriksson, D. Topgaard, U. Olsson, H. Wennerström, Microemulsions of record low amphiphile concentrations are affected by the ambient gravitational field, J. Phys. Chem. B. **120**, 6074 (2016)
103. S.A. Vitale, J.L. Katz, Liquid droplet dispersions formed by homogeneous liquid–liquid nucleation: "The Ouzo Effect", Langmuir **19**, 4105 (2003)
104. D. Stamberga, M.R. Healy, V.S. Bryantsev, C. Albisser, Y. Karslyan, B. Reinhart, A. Paulenova, M. Foster, I. Popovs, K. Lyon, B.A. Moyer, S. Jansone-Popova, Structure activity relationship approach toward the improved separation of rare-earth elements using diglycolamides, Inorg. Chem. **59**, 17620 (2020)
105. M. Špadina, K. Bohinc, T. Zemb, J.-F. Dufrêche, Synergistic solvent extraction is driven by entropy, ACS Nano. **13**, 13745 (2019)

Cite this article as: Asmae El Maangar, Tobias Lopian, Sandrine Dourdain, Werner Kunz, and Thomas Zemb. Diluent effects on the stability range of w/o micellar systems and microemulsions made with anionic extractants, EPJ Nuclear Sci. Technol. **8**, 28 (2022)